

PACS numbers: 42.81.Cn; 42.81.Gs;42.81.Pa
DOI: 10.1070/QE2009v039n03ABEH013945

Spun optical fibres: A helical structure of linear birefringence or circular birefringence?

S.K. Morshnev, V.P. Gubin, I.L. Vorob'ev, N.I. Starostin,
A.I. Sazonov, Yu.K. Chamorovsky, N.M. Korotkov

***Abstract*. An experiment has been proposed, theoretically substantiated and accomplished which has provided conclusive evidence in favour of one of two models for the behaviour of polarised light in optical fibres fabricated by spinning preforms with a high built-in linear birefringence (spun fibres): a helical structure of the built-in linear birefringence axes and circular birefringence. The experiment, carried out with a reflective fibreoptic dual-polarisation interferometer, has shown that the behaviour of polarisation states in spun fibres can be understood in terms of a helical structure of the built-in linear birefringence axes.**

Keywords: *optical fibre, birefringence, Faraday effect, spun fibre.*

1. Introduction

Magnetic-field-sensitive spun optical fibres find wide practical application, in particular in current sensors [1 – 5]. Such fibres are fabricated by spinning preforms with a sufficiently high built-in linear birefringence during the drawing process. In our opinion [3], the linear birefringence axes in spun fibres have a helical structure with a pitch determined by the fibre drawing rate and preform spin rate. Propagating in such a fibre, a light wave encounters linear birefringence axes that are rotated by an angle proportional to the distance travelled by the light. The polarisation states of the light wave vary along the fibre in a rather complicated manner. Fibre bending into a sensing coil of radius R induces an additional linear birefringence [6], which is added vectorially to the linear birefringence of the fibre with a helical structure of its axes. The polarisation state (PS) evolution in a fibre with a helical structure of its birefringence axes is of high current interest because it influences the magnetic field sensitivity of the fibre. Although such fibres have been known for more than 15 years now, there is much controversy regarding interpretation of the light polarisation evolution in them. In particular, spun fibres were assumed in several studies [1, 4, 5] to be circularly birefringent, whereas our model [3] makes it possible to interpret known results in terms of linear birefringence. We propose a decisive experiment for ascertaining whether spun fibres have a helical structure of linear birefringence or circular birefringence.

S.K. Morshnev, V.P. Gubin, I.L. Vorob'ev, N.I. Starostin, A.I. Sazonov, Yu.K. Chamorovsky, N.M. Korotkov V.A. Kotel'nikov Institute of Radio Engineering and Electronics (Fryazino Branch), Russian Academy of Sciences, pl. Vvedenskogo 1, 141190 Fryazino, Moscow region, Russia; e-mail: m137@fryazino.net, nis229@ire216.msk.su, yuchamor@online.ru

Received 11 July 2008; revision received 1 October 2008
Kvantovaya Elektronika **39** (3) 287 – 292 (2009)
Translated by O.M. Tsarev

2. Theory

In magnetic field (electric current) sensors based on the Faraday effect, two waves with orthogonal circular polarisations pass through a sensing element in the form of a magnetic-field-sensitive optical fibre. The magnetic field produces a phase difference between the waves. The difference is measured by a linear reflective interferometer [2, 3] in which all the phase differences between the orthogonal polarisations are compensated, except for that due to the Faraday effect. Because the magnetic field is a vector quantity, the Faraday-effect-induced phase shift accumulates in both directions of light propagation in the sensing element. In our model, we examine the PS evolution of a wave which is circularly polarised at the input of the sensing element. Any deviation from a purely circular polarisation reduces the magneto-optical sensitivity of the interferometer. The reason for this is that any elliptical PS can be represented as a sum of two orthogonal circular polarisations with different weights and phases, which obviously make opposite contributions to the Faraday effect.

To illustrate PS evolution, one typically resorts to the Poincare sphere representation. For our purposes, however, it is easier to find the complex-valued electric components E_x and E_y of the waves and then the corresponding point χ in the complex plane:

$$\chi = E_y/E_x. \tag{1}$$

As shown previously [7], the complex plane with points of kind (1) is a map of the Poincare sphere. Its equator projects onto the real axis of the complex plane, and the points on the equator represent linear polarisations. In particular, the point $\chi = \{0, 0\}$ corresponds to the $E \| x$ linear polarisation, and $\chi = \{\infty\}$ corresponds to the $E \| y$ linear polarisation. The poles of the Poincare sphere (circular states) project onto the points $\chi = \{0, \mathrm{j}\}$ (right-hand circular polarisation) and $\chi = \{0, -\mathrm{j}\}$ (left-hand

circular polarisation). The upper and lower half-planes correspond to right-hand and left-hand elliptically polarised states, respectively. This representation of the Poincare sphere with the complex plane implies the use of a linear polarisation basis in calculations.

Calculations were made in the differential Jones matrix approach, which reflects the continuous evolution of polarised light travelling through an anisotropic medium whose properties vary along the length of the fibre. Let the beat length of the built-in fibre linear birefringence be L_b. Over this length, the phase difference between two waves with orthogonal linear polarisations increases by 2π. Consequently, the phase difference increases with path length along the fibre at a rate $\Delta\beta = 2\pi/L_b$. The beat length of the birefringence induced by fibre bending with radius R is L_{ind}, and the phase difference increases at a rate [6]

$$\delta = 2\pi/L_{ind} = 0.2757 n_0^3 r^2/\lambda R^2, \tag{2}$$

where λ is the working wavelength; n_0 is the refractive index of the cladding; and r is the outer fibre radius. If the spin pitch is L_{tw}, the birefringence axes rotate at a rate $\xi = 2\pi/L_{tw}$. In a linear polarisation basis, the electric components E_x and E_y can be found using the differential Jones matrix for a fibre with a helical structure of its linear birefringence axes [3]:

$$\begin{bmatrix} \dfrac{dE_x}{dz} \\ \dfrac{dE_y}{dz} \end{bmatrix} = \frac{1}{2} \begin{bmatrix} j(\Delta\beta \cos 2\xi z + \delta \cos 2\varphi_0) & j(\Delta\beta \sin 2\xi z + \delta \sin 2\varphi_0) \\ j(\Delta\beta \sin 2\xi z + \delta \sin 2\varphi_0) & -j(\Delta\beta \cos 2\xi z + \delta \cos 2\varphi_0) \end{bmatrix} \begin{bmatrix} E_x \\ E_y \end{bmatrix}, \tag{3}$$

where z is the distance travelled by the light along the fibre, and φ_0 is the angle which determines the directions of the bend-induced linear birefringence axes. Using Eqns (3), one can find the complex-valued electric components E_x and E_y and determine PSs in the complex plane (χ points). Equations (3) can be reduced to a Riccati differential equation with nonharmonic coefficients, which cannot be solved in quadratures and was solved numerically.

HiBi fibres (high linear birefringence, no preform spinning). The PS evolution in HiBi fibres is illustrated in Fig. 1a. As a result of the high linear birefringence, the polarisation states shift to the equator of the Poincare sphere, then pass to the hemisphere of left-hand polarisations, pass through the pole and return to the hemisphere of right-hand polarisations, where the cycle begins anew. The polarisation state stays in the two hemispheres for equal periods of time. If, for example, a magnetic field causes the right-hand circular polarisation to be ahead of the left-hand one, then the same wave will lag in the hemisphere of left-hand polarisations. In such a fibre, the Faraday-effect-induced phase shift does not accumulate with path length.

Straight optical fibres with a helical birefringence structure. Spinning the preform (even at a moderate rate) during the fibre drawing process so that the spin pitch L_{tw} is equal to the beat length L_b has a marked effect on PS evolution (Fig. 1b): the PSs do not leave the hemisphere of right-hand polarisations and, hence, the Faraday-effect-induced phase shift accumulates along the fibre. At the same time, the deviations from the pole are rather large (the loops have a large amplitude), which implies that the net signal is considerably weaker than the signal in an ideal fibre. With decreasing the spin pitch (in Fig. 1c, the pitch L_{tw} is half the beat length L_b), the deviation from the pole decreases substantially and, hence, the magneto-optical response of the sensor rises. If a straight fibre is used in a sensing element, its sensitivity can be enhanced by merely reducing the spin pitch L_{tw}.

Optical fibres with a helical birefringence structure, wound onto a spool of constant radius. In most applications, the fibre must be coiled with a particular radius in order to enhance the absolute magneto-optical response of the sensor. The PS evolution in a sensing element in the form of an optical fibre that has a helical birefringence structure and is wound onto a spool of a relatively large radius, $R = 18$ mm ($L_{ind} = 973$ mm at $\lambda = 1.55$ μm), is illustrated in Fig. 2a. The picture resembles the motion of the angular momentum vector of a gyroscope involved in

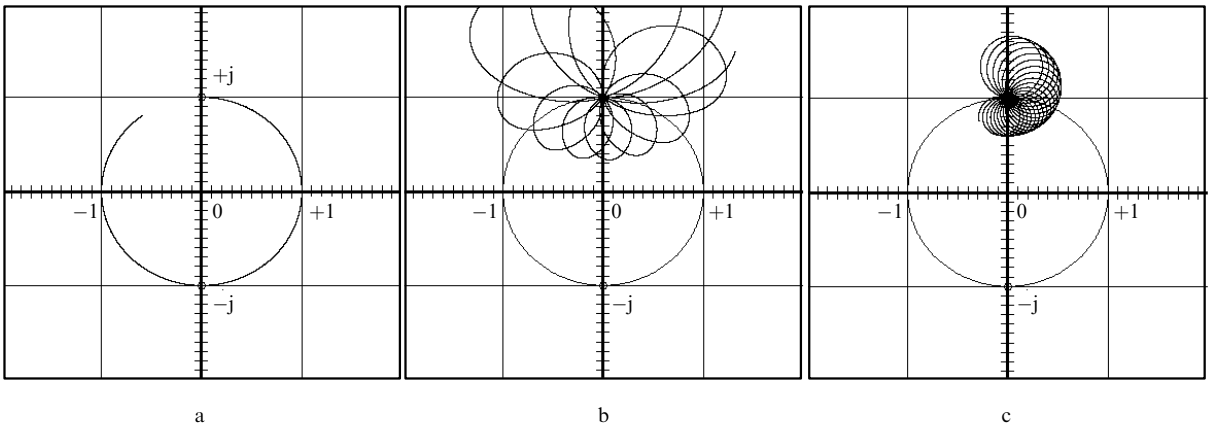

Figure 1. Evolution of polarisation states in the complex plane for (a) an unspun highly linearly birefringent fibre and (b, c) straight fibres with a helical birefringence structure (beat length of the built-in linear birefringence $L_b = 16$ mm); spin pitch $L_{tw} = 16$ (b) and (c) 8 mm.

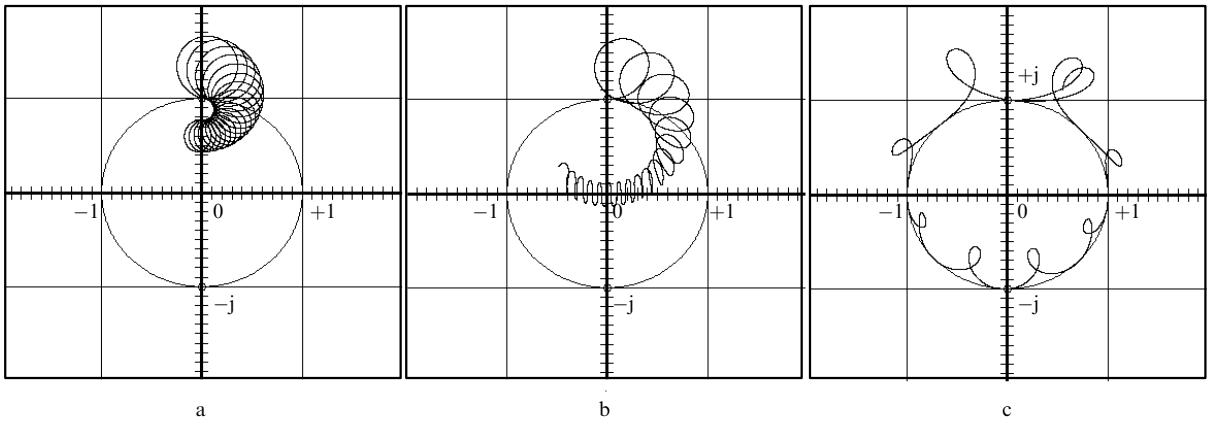

Figure 2. Evolution of polarisation states in fibres with a helical structure of linear birefringence ($L_b = 16$ mm, $L_{tw} = 8$ mm) wound onto spools with $R = 18$ (a), (b) 7.3 and (c) 3.25 mm.

precession (envelope circle) and nutation oscillations (loops touching the envelope circle). To differentiate between the two well-defined kinds of PS evolution, we will use the term 'nutation'. One can see that here not all of the nutation loops pass through the pole and that their envelope is a circle. Let us reduce the bending radius. At $R = 7.3$ mm ($L_{ind} = 160$ mm), the PS evolution has the form represented in Fig. 2b. The envelope circle is such that some of the PSs lie beyond the northern hemisphere, and the sensitivity drops sharply. It should be emphasised that this occurs at $L_{ind} = 160$ mm, i.e. at an induced birefringence an order of magnitude lower than the intrinsic one ($L_b = 16$ mm). Further displacement to the southern hemisphere is observed at $L_{ind}/L_b = 2$ and a bending radius $R =$ 3.25 mm (Fig. 2c). Clearly, at this bending radius the Faraday-effect-induced phase shift will not accumulate along the fibre (cf. Fig. 1a).

If the spin pitch and bending radius are maintained constant at $L_{tw} = 4$ mm and $R = 10.3$ mm, then at a beat length of the built-in linear birefringence $L_b = 16$ mm the PSs reach the equator of the Poincare sphere (Fig. 3a). Increasing the built-in fibre linear birefringence by a factor of 1.25 ($L_b = 12$ mm), we obtain the PS evolution represented in Fig. 3b. As seen, the increase in built-in linear birefringence enhances the sensitivity: here the PS's do not reach the equator. Further increasing the intrinsic fibre birefringence reduces the radius of the envelope circle. Thus, the built-in fibre linear birefringence is obviously involved in the suppression of the linear birefringence induced by winding the fibre onto a spool of constant radius.

Figure 4 illustrates the effect of the spin pitch on the PS evolution in spun fibres with a beat length of the intrinsic linear birefringence $L_b = 16$ mm, wound onto spools of radius $R = 10.3$ mm ($L_{ind} \approx 300$ mm). As seen, reducing the pitch from $L_{tw} = 8$ mm (Fig. 4a) to $L_{tw} = 2$ mm (Fig. 4c) reduces the nutation amplitude, as in the case of straight fibres, but in this sequence the radius of the envelope circle increases more rapidly, and the PSs reach the southern hemisphere. Clearly, fibre spinning does not contribute to the suppression of the linear birefringence resulting from fibre bending.

The situation is paradoxical: on the one hand, the Faraday effect cannot be observed without fibre spinning, but on the other, too rapid spinning in combination with bending reduces the sensitivity. This can be rationalised as follows: spinning suppresses the intrinsic fibre linear birefringence but cannot suppress the bend-induced linear birefringence. Therefore, the effect of bending is suppressed with direct participation of the built-in linear birefringence. At small spin pitches, the built-in linear birefringence is strongly suppressed and becomes insufficient to supress the bend-induced birefringence.

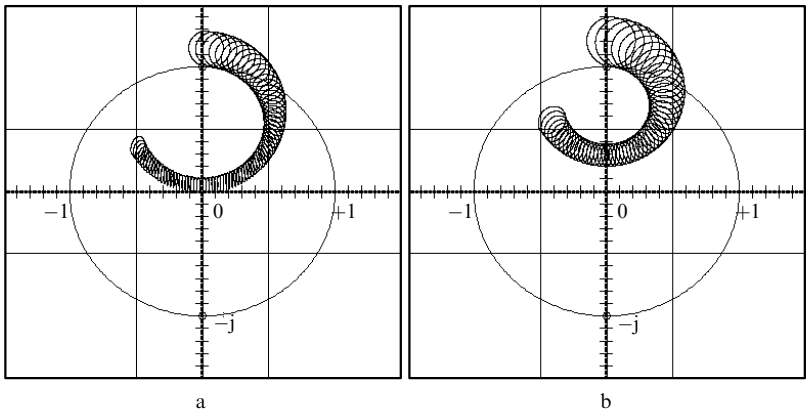

Figure 3. Evolution of polarisation states in fibres with a helical structure of linear birefringence ($L_{tw} = 4$ mm) wound onto spools of radius $R = 10.3$ mm. The beat length of the built-in linear birefringence is $L_b = 16$ (a) and 12 mm (b).

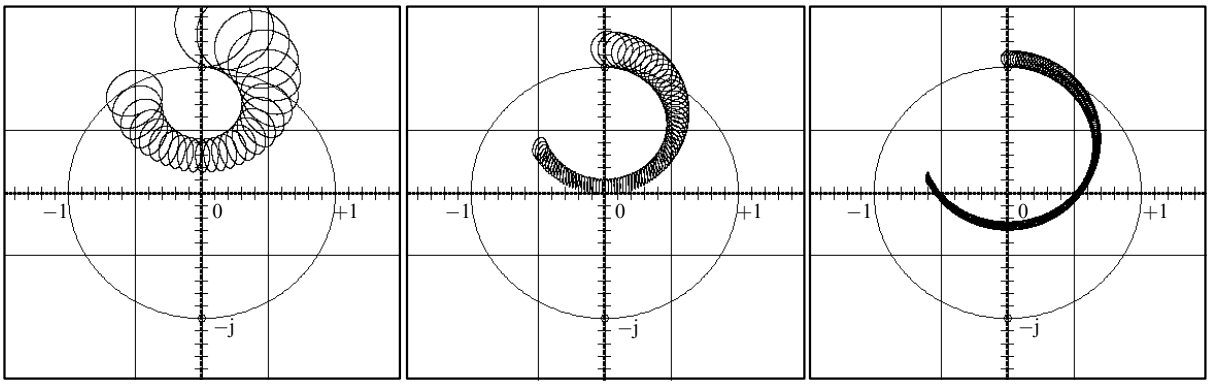

Figure 4. Evolution of polarisation states in fibres with a helical structure of linear birefringence ($L_b = 16$ mm) wound onto spools of radius $R =$ 10.3 mm. The spin pitch is $L_{tw} = 8$ (a), (b) 4 and (c) 2 mm.

It should be emphasised that our calculation results differ significantly from results obtained in the commonly accepted model [1, 4], in which preform spinning is believed to result in circular birefringence. The key distinctive feature of circular birefringence is that it is orthogonal to all linear birefringences regardless of their nature. Reducing the spin pitch must increase circular birefringence and, hence, lead to more effective suppression of any linear birefringence, including that arising at constant bending radius. LoBi fibres (low intrinsic linear birefringence) prepared by spinning preforms at a small pitch ($\sim$4 mm) and then wound onto spools of various radii exhibit a phase delay exactly equal to that resulting from the bend-induced linear birefringence, with no evidence of circular birefringence.

Moreover, built-in circular birefringence in a spun fibre would lead to an elliptical eigenstate of the fibre: if such a PS will be launched into the fibre, then, independent of the fibre length, the same state will emerge at the fibre output (e.g. linear polarisation in HiBi fibres). Evolution curves demonstrate that, in our model, even straight fibres have no elliptical eigenstates: the PS varies along the fibre.

To clarify this issue, we propose the following experiment. An interferometric sensing element should incorporate two fibres with built-in birefringence which have the same beat length, e.g. $L_b = 15$ mm, but differ in spin pitch, e.g. $L_{1tw} = 2.5$ mm and $L_{2tw} = 7.5$ mm. The relative response of the sensor, S/S_{id}, should be measured as a function of fibre bending radius R in the sensing element (S_{id} is the response of a sensor with a sensing element fabricated from an ideal, isotropic fibre). As in the case of straight fibres, at large bending radii ($R \sim 40$ mm) the sensitivity of the fibre with the smaller pitch, L_{1tw}, will exceed that of the fibre with the larger pitch, L_{2tw}. At the same time, as shown above a structure with a smaller spin pitch is more effective in suppressing the built-in linear birefringence, which however plays a key role in suppressing the bend-induced linear birefringence. Therefore, reducing the fibre bending radius R in the sensing element will reduce the sensitivity of the fibre with pitch L_{1tw} more rapidly compared to the fibre with pitch L_{2tw}. At low values of R, the relative sensitivity S/S_{id} of the fibre with the smaller pitch will be lower than that of the fibre with the larger pitch.

This behaviour differs radically from that of circularly birefringent fibres. If circular birefringence can suppress the built-in fibre linear birefringence ($L_b \sim 16$ mm), enabling the Faraday-effect-induced phase shift to accumulate along the fibre, it will no doubt suppress the linear birefringence induced by bending with $R = 10$ mm ($L_{ind} \approx 300$ mm). In the range 10 mm $\leqslant R \leqslant$ 40 mm, relative sensitivity S/S_{id} will vary insignificantly. The plots of S/S_{id} versus R for two fibres differing in the beat length of circular birefringence will be parallel to one another, with no intersection.

The proposed experiment is considerably complicated by the uncontrolled value of φ_0 [see Eqn. (3)]. This is the angle between the fast (or slow) axes of the intrinsic and bend-induced linear birefringences at the input of the bent part of the fibre. Clearly, it has a rather random value, but it influences the relative sensitivity of the fibre. We calculated S/S_{id} as a function of φ_0 in the range $0 \leqslant \varphi_0 \leqslant \pi/2$. In this range, S/S_{id} varies by approximately 2 % at large bending radii. At $R \sim 10$ mm, the spread is almost 20 % in fibres with $L_{2tw} = 7.5$ mm and 2 % – 10 % in fibres with $L_{1tw} =$ 2.5 mm.

The uncontrolled parameter can be eliminated from the experiment by heating the coil. As a result of heating, the fibre elongates, which leads to rotation of the built-in linear birefringence axes relative to the axes of the linear birefringence induced by bending with a preset radius at the input of the coil. Its sensitivity varies sinusoidally, and one can determine the maximum and minimum values of its relative sensitivity S/S_{id}. The contributions of other mechanisms to the variation in S/S_{id} are within 1 %.

The above is illustrated in Fig. 5, which plots S/S_{id} versus the bending radius R of the fibre in the sensing element of a current sensor. For two fibres with a helical structure of linear birefringence, having the same beat length, $L_b = 15$ mm, but differing in spin pitch L_{tw}, we obtained two pairs of intersecting theoretical curves, marked by filled and open rhombuses ($L_{1tw} = 2.5$ mm) and triangles ($L_{2tw} = 7.5$ mm). The filled and open data points show, respectively, the maximum ($\varphi_0 = \pi/2$) and minimum ($\varphi_0 = 0$) values of S/S_{id}.

One can see in Fig. 5 that, at $R = 36$ mm, the minimum relative sensitivity S/S_{id} of the fibre with $L_{1tw} = 2.5$ mm is approximately 3 % higher than the maximum sensitivity S/S_{id} of the fibre with $L_{2tw} = 7.5$ mm and, hence, can be resolved in experiment. At $R = 10$ mm, the maximum relative sensitivity of the fibre with $L_{1tw} = 2.5$ mm is

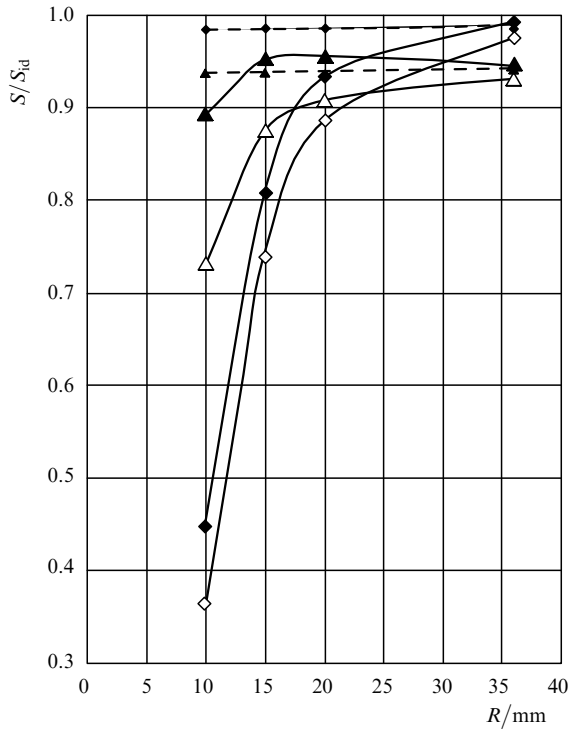

Figure 5. Relative sensitivity S/S_{id} as a function of fibre bending radius R for a current sensor with a sensing element made from coiled fibres with a helical birefringence structure: $L_b = 15$ mm, $L_{1tw} = 2.5$ mm (◇,◆), $L_{2tw} = 7.5$ mm (△,▲). The filled data points show the maximum relative sensitivity ($\varphi_0 = \pi/2$), and the open data points show the minimum sensitivity ($\varphi_0 = 0$). The dashed lines show S/S_{id} as a function of R for circularly birefringent spun fibres; the small rhombuses and triangles represent fibres with $L_{1tw} = 2.5$ mm and $L_{2tw} = 7.5$ mm, respectively.

substantially lower than the minimum sensitivity of the fibre with $L_{2tw} = 7.5$ mm.

3. Experimental

Figure 6 schematically shows the experimental setup used, which includes a linear reflective fibreoptic dual-polarisation interferometer (FDI) for electric current measurements using the Faraday effect in a silica fibre [2, 3]. The sensing element of the FDI consists of the coil to be studied, fusion-spliced to the output fibre pigtail of a quarter-wave plate. Eight coils of various diameters were fabricated from two types of spun fibres which had the same beat length of the built-in linear birefringence ($L_b = 15$ mm) but differed in spin pitch ($L_{tw} = 2.5$ and 7.5 mm). The fibres were wound at 7-g tension onto Plexiglas spools of radii 36, 20, 15 and 10 mm. To raise the effective current across the coil plane, each fibre coil had a toroidal copper wire winding. The number of turns in each coil was $N = 160$, and the number of copper wire turns was $M = 36$. As the FDI mirror, we used the fibre end-face, cleaved perpendicular to the fibre axis. Each coil had input (*3*) and output (*4*) straight fibre ends ~50 cm in length. In sensitivity measurements, a standard current $I_0 = 3$ A was passed through the copper winding. The other parts of the FDI were identical to those described previously and will not be considered here. The FDI signal processing unit analysed ratios of modulation harmonics [3], ensuring a measurement accuracy of ±0.1 %.

The magneto-optical sensitivity S_i of the ith coil was measured using the following procedure. First, the FDI visibility was maximised by slightly deforming the fibre ends at $I_0 = 0$. The highest value of S_i was obtained in the case of circular polarisation at the input of the coil. Next, a current $I_0 = 3$ A was turned on, and the measured current signal was recorded.

According to the above theory, the sensitivity of a fibre depends on the angle φ_0 between the built-in and bend-induced linear birefringence axes. This angle varies because the current being measured heats the fibre coil. As a result, the measured current signal I_i oscillates in time. To determine the magneto-optical sensitivity S_i of the coils ($S_i = I_i/I_0$), we used the maximum values of I_i. Since the sensitivity (scale factor of the current sensor) depends not only on the coil parameters but also on the other optical components of the FDI, the current sensor was calibrated at a coil radius of 36 mm and $L_{1tw} = 2.5$ mm. At these coil parameters, the system exhibited the highest sensitivity under the conditions of our experiments, with a relative

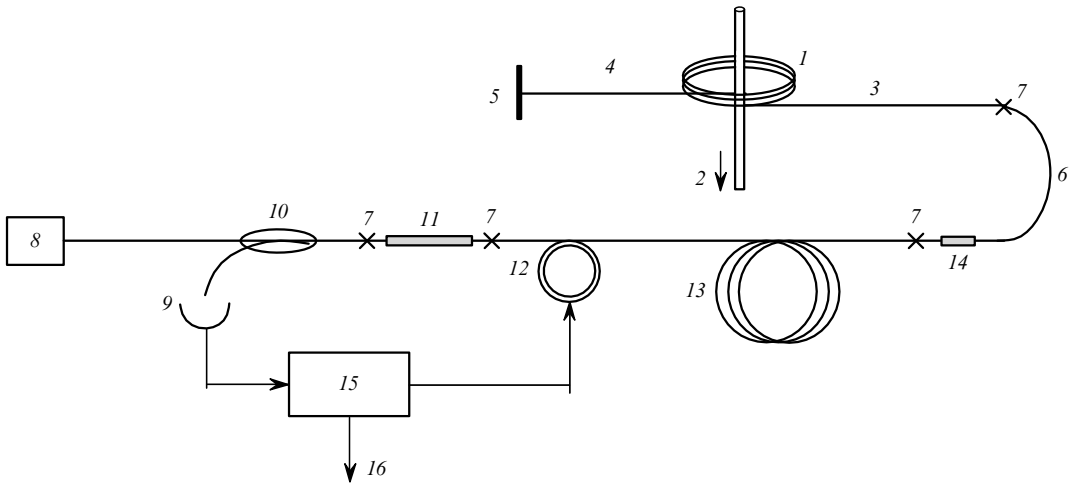

Figure 6. Schematic of the experimental setup: (*1*) coil to be studied, (*2*) wire carrying a standard current; (*3*, *4*) input and output ends of the coil, respectively; (*5*) mirror; (*6*) output fibre pigtail of the wave plate; (*7*) fibre splices; (*8*) light source; (*9*) photodetector; (*10*) directional coupler; (*11*) polariser; (*12*) polarisation modulator; (*13*) fibre delay line; (*14*) quarter-wave plate; (*15*) electronic unit; (*16*) measured current.

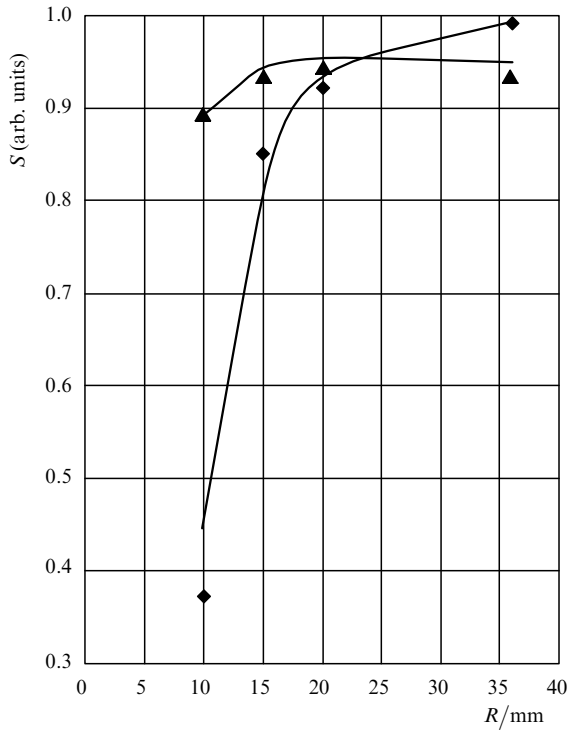

Figure 7. Magneto-optical sensitivity as a function of the bending radius R of spun fibres with $L_b = 15$ mm at spin pitches $L_{1tw} = 2.5$ mm (◆) and $L_{2tw} = 7.5$ mm (▲). The points represent the experimental data, and the solid lines represent the calculation results.

value of 0.99, in agreement with the theoretical value for these parameters (Fig. 5). In this way, the experimental data were matched to the theoretical predictions.

The measured magneto-optical sensitivity of the system as a function of the bending radius R of spun fibres is presented in Fig. 7. Note that there is good agreement between theory and experiment at both high and low values of R.

It follows from both theory and experiment that, at high values of R, the spun fibres with pitch L_{1tw} offer higher sensitivity, which approaches that of an ideal (isotropic) fibre. At the same time, as the bending radius decreases, the sensitivity of these fibres drops more rapidly than that of the fibres with pitch L_{2tw}, which indicates according to theory that the latter fibres are more stable to bending deformation.

4. Conclusions

The present experimental data for elastically bent (with various radii) optical fibres fabricated by spinning preforms with a high built-in linear birefringence (spun fibres) provides conclusive evidence in favour of one of the two models for spun fibres: a helical structure of the built-in linear birefringence. The experimental curves of magneto-optical sensitivity versus bending radius R for two samples of spun fibres with the same linear birefringence beat length ($L_b = 15$ mm) and different spin pitches ($L_{1tw} = 2.5$ mm, $L_{2tw} = 7.5$ mm) were found to intersect, in agreement with theoretical predictions. The sensitivity of the fibre with the smaller pitch is higher at larger bending radii and drops precipitously with decreasing R. The fibre with the larger pitch exhibits higher sensitivity at smaller bending radii. Spinning the preform during the drawing process suppresses only the built-in linear birefringence, which may then become too low ($L_{1tw} = 2.5$ mm) to suppress the linear birefringence induced by fibre bending with small radius R.

The model commonly accepted at present [1, 4], in which preform spinning is believed to result in circular birefringence, is fundamentally inconsistent with the observed intersection of the sensitivity versus bending radius curves because the major cause of bend-induced birefringence suppression in that model is circular birefringence, which obviously increases with decreasing the spin period.

Thus, our experimental data lead us to conclude that spun fibres are adequately modelled by a helical structure of built-in linear birefringence.

References

1. Laming R.I., Payne D.N. *J. Lightwave Technol.*, **7**, 2084 (1989).
2. Polynkin P., Blake J. *J. Lightwave Technol.*, **23** (11), 3815 (2005).
3. Gubin V.P., Isaev V.A., Morshnev S.K., Sazonov A.I., Starostin N.I., Chamorovsky Yu.K., Oussov A.I. *Kvantovaya Elektron.*, **36** (3), 287 (2006) [*Quantum. Electron.*, **36** (3), 287 (2006)].
4. Dakin J., Culshaw B. (Eds.) *Optical Fiber Sensors: Principles and Components* (Boston: Artech House, 1988).
5. Michie A., Canning J., Bassett I., Haywood J., Digweed K., Aslund M., Ashton B., Stevenson M., Digweed J., Lau A., Scandurra D. *Opt. Express*, **15** (4), 1811 (2007).
6. Rashleigh S.C. *J. Lightwave Technol.*, **1**, 312 (1983).
7. Azzam R.M.A., Bashara N.M. *Ellipsometry and Polarised Light* (Amsterdam – New York – Oxford: North-Holland Publ. Comp., 1977).